A WINDOWED GRAPH FOURIER TRANSFORM

David I Shuman[1]*, Benjamin Ricaud*[2]*, and Pierre Vandergheynst*[1]

[1]Ecole Polytechnique Fédérale de Lausanne (EPFL), Lausanne, Switzerland
[2]Aix-Marseille University, Marseille, France
Email: david.shuman@epfl.ch, bricaud@cmi.univ-mrs.fr, pierre.vandergheynst@epfl.ch

ABSTRACT

The prevalence of signals on weighted graphs is increasing; however, because of the irregular structure of weighted graphs, classical signal processing techniques cannot be directly applied to signals on graphs. In this paper, we define generalized translation and modulation operators for signals on graphs, and use these operators to adapt the classical windowed Fourier transform to the graph setting, enabling vertex-frequency analysis. When we apply this transform to a signal with frequency components that vary along a path graph, the resulting spectrogram matches our intuition from classical discrete-time signal processing. Yet, our construction is fully generalized and can be applied to analyze signals on any undirected, connected, weighted graph.

***Index Terms*—** Signal processing on graphs, time-frequency analysis, generalized translation and modulation, spectral graph theory

1. INTRODUCTION

In an increasing number of applications such as social networks, electricity networks, transportation networks, and sensor networks, data naturally reside on the vertices of weighted graphs. Moreover, weighted graphs are a flexible tool that can be used to describe similarities between data points in statistical learning problems, functional connectivities between different regions of the brain, and the geometric structures of countless other topologically-complicated data domains. Unfortunately, weighted graphs are irregular structures that lack a shift-invariant notion of translation, a key component in many signal processing techniques for data on regular Euclidean spaces. Thus, the existing techniques cannot be directly applied to signals on graphs, and an important challenge is to design localized transform methods to efficiently extract information from high-dimensional data on graphs (either statistically or visually), as well as to regularize ill-posed inverse problems. Accordingly, a number of new multiscale wavelet transforms for signals on graphs have been introduced recently (see, e.g., the introductions of [1, 2] for up-to-date reviews of these wavelet transforms).

Another important class of time-frequency analysis tools in classical signal processing are windowed Fourier transforms, also called short-time Fourier transforms. Windowed Fourier transforms are particularly useful in extracting information from signals with oscillations that are localized in time or space. Such signals appear frequently in applications such as audio and speech processing, vibration analysis, and radar detection.

Underlying the classical windowed Fourier transform are the translation and modulation operators. While these fundamental operations seem simple in the classical setting, they become significantly more challenging when we deal with signals on graphs. For example, when we want to translate the blue Mexican hat wavelet on the real line in Figure 1(a) to the right by 5, the result is the dashed red signal. However, it is not immediately clear what it means to translate the blue signal in Figure 1(c) on the weighted graph in Figure 1(b) "to vertex 1000." Modulating a signal on the real line by a complex exponential corresponds to translation in the Fourier domain. However, the analogous spectrum in the graph setting is discrete and bounded, and therefore it is difficult to define a modulation in the vertex domain that corresponds to translation in the graph spectral domain.

In this paper, we define generalized translation and modulation operators for signals on graphs, and use these operators to adapt the classical windowed Fourier transform to the graph setting, enabling vertex-frequency analysis.

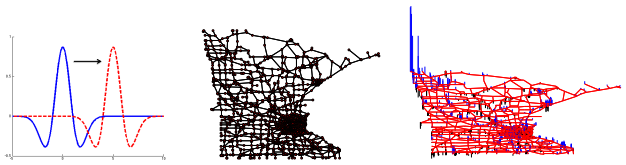

(a) (b) (c)

Fig. 1. (a) Classical translation. (b) The Minnesota road graph. (c) What does it mean to "translate" this signal on the vertices of the Minnesota road graph?

2. THE CLASSICAL WINDOWED FOURIER TRANSFORM

For any $f \in L^2(\mathbb{R})$ and $u \in \mathbb{R}$, the translation operator $T_u : L^2(\mathbb{R}) \to L^2(\mathbb{R})$ is defined by

$$(T_u f)(t) := f(t-u), \tag{1}$$

and for any $\xi \in \mathbb{R}$, the modulation operator $M_\xi : L^2(\mathbb{R}) \to L^2(\mathbb{R})$ is defined by

$$(M_\xi f)(t) := e^{2\pi i \xi t} f(t). \tag{2}$$

Now let $g \in L^2(\mathbb{R})$ be a window with $\|g\|_2 = 1$. Then a windowed Fourier atom (see, e.g., [3, Chapter 4.2]) is given by

$$g_{u,\xi}(t) := (M_\xi T_u g)(t) = g(t-u)e^{2\pi i \xi t}, \tag{3}$$

and the windowed Fourier transform of a function $f \in L^2(\mathbb{R})$ is

$$Sf(u,\xi) := \langle f, g_{u,\xi} \rangle = \int_{-\infty}^{\infty} f(t)\overline{g(t-u)}e^{-2\pi i \xi t} dt. \tag{4}$$

This work was supported by FET-Open grant number 255931 UNLocX.

3. SPECTRAL GRAPH THEORY NOTATION

We consider undirected, connected, weighted graphs $\mathcal{G} = \{\mathcal{V}, \mathcal{E}, W\}$, where $\mathcal{V}$ is a finite set of vertices with $|\mathcal{V}| = N$, $\mathcal{E}$ is a set of edges, and W is a weighted adjacency matrix (see, e.g., [4] for all definitions in this section). A signal $f : \mathcal{V} \to \mathbb{R}^N$ defined on the vertices of the graph may be represented as a vector $f \in \mathbb{R}^N$, where the n^{th} component of the vector f represents the signal value at the n^{th} vertex in $\mathcal{V}$. The non-normalized graph Laplacian is defined as $\mathcal{L} := D - W$, where D is the diagonal degree matrix.

As the graph Laplacian $\mathcal{L}$ is a real symmetric matrix, it has a complete set of orthonormal eigenvectors, which we denote by $\{\chi_\ell\}_{\ell=0,1,\ldots,N-1}$. Without loss of generality, we assume that the associated real, non-negative Laplacian eigenvalues are ordered as $0 = \lambda_0 < \lambda_1 \leq \lambda_2 ... \leq \lambda_{N-1} := \lambda_{\max}$.

The classical Fourier transform is the expansion of a function f in terms of the eigenfunctions of the Laplace operator, i.e., $\hat{f}(\xi) = \langle f, e^{2\pi i \xi t} \rangle$. Analogously, the *graph Fourier transform* $\hat{f}$ of a function $f \in \mathbb{R}^N$ on the vertices of $\mathcal{G}$ is the expansion of f in terms of the eigenfunctions of the graph Laplacian. It is defined by $\hat{f}(\ell) := \langle f, \chi_\ell \rangle = \sum_{n=1}^{N} \chi_\ell^*(n) f(n)$, where we adopt the convention that the inner product be conjugate-linear in the second argument. The *inverse graph Fourier transform* is then given by $f(n) = \sum_{\ell=0}^{N-1} \hat{f}(\ell)\chi_\ell(n)$.

4. GENERALIZED TRANSLATION

For signals $f, g \in L^2(\mathbb{R})$, the convolution product $h = f * g$ satisfies

$$h(t) = (f * g)(t) = \int_{\mathbb{R}} \hat{h}(\xi) e^{2\pi i \xi t} d\xi = \int_{\mathbb{R}} \hat{f}(\xi)\hat{g}(\xi)\psi_\xi(t) d\xi, \quad (5)$$

where $\psi_\xi(t) = e^{2\pi i \xi t}$. By replacing the complex exponentials in (5) with the graph Laplacian eigenvectors, we define a *generalized convolution* of signals $f, g \in \mathbb{R}^N$ on a graph by

$$(f * g)(n) := \sum_{\ell=0}^{N-1} \hat{f}(\ell)\hat{g}(\ell)\chi_\ell(n). \quad (6)$$

Now the application of the classical translation operator T_u defined in (1) to a function $f \in L^2(\mathbb{R})$ can be seen as a convolution with δ_u:

$$(T_u f)(t) := f(t-u) = (f * \delta_u)(t) \overset{(5)}{=} \int_{\mathbb{R}} \hat{f}(\xi)\widehat{\delta_u}(\xi)\psi_\xi(t) d\xi = \int_{\mathbb{R}} \hat{f}(\xi)\psi_\xi^*(u)\psi_\xi(t) d\xi,$$

where the equalities are in the weak sense. Thus, for any signal $f \in \mathbb{R}^N$ defined on the the graph $\mathcal{G}$ and any $i \in \{1, 2, \ldots, N\}$, we also define a *generalized translation operator* $T_i : \mathbb{R}^N \to \mathbb{R}^N$ via generalized convolution with a delta centered at vertex i:

$$(T_i f)(n) := \sqrt{N}(f * \delta_i)(n) \overset{(6)}{=} \sqrt{N} \sum_{\ell=0}^{N-1} \hat{f}(\ell)\chi_\ell^*(i)\chi_\ell(n). \quad (7)$$

In Figure 2, we apply generalized translation operators to the graph signal from Figure 1(c).

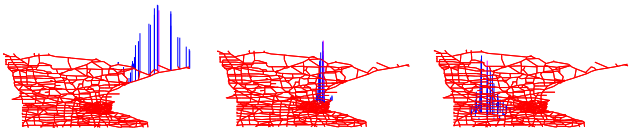

(a) (b) (c)

Fig. 2. The translated signals (a) $T_{200}f$, (b) $T_{1000}f$, and (c) $T_{2000}f$, where f, the signal shown in Figure 1(c), is a normalized heat kernel satisfying $\hat{f}(\ell) = Ce^{-5\lambda_\ell}$.

5. GENERALIZED MODULATION

Motivated by the fact that the classical modulation (2) is a multiplication by a Laplacian eigenfunction, we define, for any $k \in \{0, 1, \ldots, N-1\}$, a *generalized modulation operator* $M_k : \mathbb{R}^N \to \mathbb{R}^N$ by

$$(M_k f)(n) := \sqrt{N} f(n)\chi_k(n).$$

First, note that M_0 is the identity operator, as $\chi_0(n) = \frac{1}{\sqrt{N}}$ for all n for connected graphs. In the classical case, the modulation operator represents a translation in the Fourier domain:

$$\widehat{M_\xi f}(\omega) = \hat{f}(\omega - \xi), \forall \omega \in \mathbb{R}.$$

This property is not true in general for our modulation operator on graphs due to the discrete nature of the graph. However, we do have the nice property that if $\hat{g}(\ell) = \delta_0(\lambda_l)$, then

$$\widehat{M_k g}(\ell) = \sum_{n=1}^{N} \chi_\ell^*(n)(M_k g)(n) = \sum_{n=1}^{N} \chi_\ell^*(n)\sqrt{N}\chi_k(n)\frac{1}{\sqrt{N}} = \delta_0(\lambda_\ell - \lambda_k),$$

so M_k maps the DC component of any signal $f \in \mathbb{R}^N$ to $\hat{f}(0)\chi_k$. Moreover, if we start with a function f that is localized around the eigenvalue 0 in the graph spectral domain, as in Figure 3, then $M_k f$ will be localized around the eigenvalue λ_k in the graph spectral domain. We quantify this localization in the next theorem.

Theorem 1: *Given a weighted graph $\mathcal{G}$ with N vertices, let $C_1(\mathcal{G})$ be a constant such that*

$$\max_{\substack{\ell = 0, 1, \ldots, N-1 \\ i = 1, 2, \ldots, N}} \{|\chi_\ell(i)|\} \leq \frac{C_1}{\sqrt{N}}. \quad (8)$$

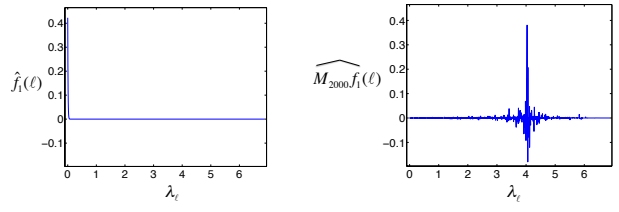

(a) (b)

Fig. 3. (a) The graph spectral representation of a signal f_1 with $\hat{f}_1(\ell) = Ce^{-100\lambda_\ell}$, where the constant C is chosen such that $\|f_1\|_2 = 1$. (b) The graph spectral representation $\widehat{M_{2000}f_1}$ of the modulated signal $M_{2000}f_1$. Note that $\lambda_{2000} = 4.03$.

If for some $\kappa > 0$, a given signal f satisfies

$$\frac{1}{|\hat{f}(0)|}\sum_{\ell=1}^{N-1}|\hat{f}(\ell)| \leq \frac{1}{C_1 + \kappa(C_1)^3}, \tag{9}$$

then

$$|\widehat{M_k f}(k)| \geq \kappa |\widehat{M_k f}(\ell)| \text{ for all } \ell \neq k. \tag{10}$$

Proof.

$$\begin{aligned}
&\widehat{M_k f}(\ell') \\
&= \sum_{n=1}^{N} \sqrt{N}\chi^*_{\ell'}(n)\chi_k(n)f(n) \\
&= \sum_{n=1}^{N} \sqrt{N}\chi^*_{\ell'}(n)\chi_k(n)\sum_{\ell''=0}^{N-1}\chi_{\ell''}(n)\hat{f}(\ell'') \\
&= \sum_{n=1}^{N} \sqrt{N}\chi^*_{\ell'}(n)\chi_k(n)\left[\frac{\hat{f}(0)}{\sqrt{N}} + \sum_{\ell''=1}^{N-1}\chi_{\ell''}(n)\hat{f}(\ell'')\right] \\
&= \hat{f}(0)\delta_{\ell' k} + \sum_{n=1}^{N} \sqrt{N}\chi^*_{\ell'}(n)\chi_k(n)\sum_{\ell''=1}^{N-1}\chi_{\ell''}(n)\hat{f}(\ell''). \qquad (11)
\end{aligned}$$

Therefore, we have

$$\begin{aligned}
&|\widehat{M_k f}(k)| \\
&= \left|\hat{f}(0) + \sum_{n=1}^{N}\sqrt{N}|\chi_k(n)|^2\sum_{\ell''=1}^{N-1}\chi_{\ell''}(n)\hat{f}(\ell'')\right| \\
&\geq |\hat{f}(0)| - \left|\sum_{n=1}^{N}\sqrt{N}|\chi_k(n)|^2\sum_{\ell''=1}^{N-1}\chi_{\ell''}(n)\hat{f}(\ell'')\right| \\
&\geq |\hat{f}(0)| - \sum_{n=1}^{N}\sqrt{N}|\chi_k(n)|^2\sum_{\ell''=1}^{N-1}|\chi_{\ell''}(n)|\,|\hat{f}(\ell'')| \\
&\geq |\hat{f}(0)| - C_1\sum_{\ell''=1}^{N-1}|\hat{f}(\ell'')| \\
&\geq |\hat{f}(0)|\left(1 - \frac{C_1}{C_1 + \kappa(C_1)^3}\right), \qquad (12)
\end{aligned}$$

where the last two inequalities follow from (8) and (9), respectively. Returning to (11) for $\ell \neq k$, we have

$$\begin{aligned}
\kappa|\widehat{M_k f}(\ell)| &= \kappa\left|\sum_{n=1}^{N}\sqrt{N}\chi^*_{\ell}(n)\chi_k(n)\sum_{\ell''=1}^{N-1}\chi_{\ell''}(n)\hat{f}(\ell'')\right| \\
&\leq \kappa\sum_{n=1}^{N}\sum_{\ell''=1}^{N-1}\sqrt{N}\,|\chi^*_{\ell}(n)\chi_k(n)\chi_{\ell''}(n)|\,|\hat{f}(\ell'')| \\
&\leq \kappa C_1^3\sum_{\ell''=1}^{N-1}|\hat{f}(\ell'')| \\
&\leq |\hat{f}(0)|\frac{\kappa C_1^3}{C_1 + \kappa C_1^3}, \qquad (13)
\end{aligned}$$

where the last two inequalities once again follow from (8) and (9), respectively. Combining (12) and (13) yields (10). □

6. WINDOWED GRAPH FOURIER FRAMES

Analogously to (3) and (4) in the classical case, for a window $g \in \mathbb{R}^N$, we define a windowed graph Fourier atom by

$$g_{i,k}(n) := (M_k T_i g)(n) = N\chi_k(n)\sum_{\ell=0}^{N-1}\hat{g}(\ell)\chi^*_{\ell}(i)\chi_{\ell}(n),$$

and the windowed graph Fourier transform of a function $f \in \mathbb{R}^N$ by

$$Sf(i,k) := \langle f, g_{i,k}\rangle.$$

Theorem 2: *If $\hat{g}(0) \neq 0$, then $\{g_{i,k}\}_{i=1,2,\ldots,N;\ k=0,1,\ldots,N-1}$ is a frame with lower frame bound*

$$A := \min_{n\in\{1,2,\ldots,N\}}\left\{N\|T_n g\|_2^2\right\},$$

and upper frame bound

$$B := \max_{n\in\{1,2,\ldots,N\}}\left\{N\|T_n g\|_2^2\right\}.$$

Proof.

$$\begin{aligned}
\sum_{i=1}^{N}\sum_{k=0}^{N-1}|\langle f, g_{i,k}\rangle|^2 &= \sum_{i=1}^{N}\sum_{k=0}^{N-1}|\langle f, M_k T_i g\rangle|^2 \\
&= N\sum_{i=1}^{N}\sum_{k=0}^{N-1}|\langle f(T_i g)^*, \chi_k\rangle|^2 \\
&= N\sum_{i=1}^{N}\langle f(T_i g)^*, f(T_i g)^*\rangle \qquad (14) \\
&= N\sum_{i=1}^{N}\sum_{n=1}^{N}|f(n)|^2\,|(T_i g)(n)|^2 \\
&= N\sum_{i=1}^{N}\sum_{n=1}^{N}|f(n)|^2\,|(T_n g)(i)|^2 \qquad (15) \\
&= N\sum_{n=1}^{N}|f(n)|^2\,\|T_n g\|_2^2, \qquad (16)
\end{aligned}$$

where (14) is due to Parseval's identity, and (15) follows from the symmetry of $\mathcal{L}$ and the definition (7) of T_i. Moreover, under the hypothesis that $\hat{g}(0) \neq 0$, we have

$$\|T_n g\|_2^2 = N\sum_{\ell=0}^{N-1}|\hat{g}(\ell)|^2\,|\chi_l(n)|^2 \geq |\hat{g}(0)|^2 > 0. \tag{17}$$

Combining (16) and (17), for $f \neq 0$,

$$0 < A\|f\|_2^2 \leq \sum_{i=1}^{N}\sum_{k=0}^{N-1}|\langle f, g_{i,k}\rangle|^2 \leq B\|f\|_2^2 < \infty.$$

□

7. EXAMPLES

We now present three examples to provide further intuition behind the proposed windowed graph Fourier transform. In the first example, we consider a path graph of 180 vertices, with all the weights equal to one. The graph Laplacian eigenvectors for the path graph

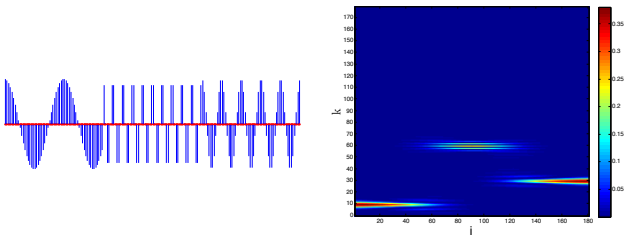

(a) (b)

Fig. 4. (a) A signal f on the path graph that is comprised of three different graph Laplacian eigenvectors restricted to three different segments of the graph. (b) A spectrogram of f. The vertex indices are on the horizontal axis, and the frequency indices are on the vertical axis.

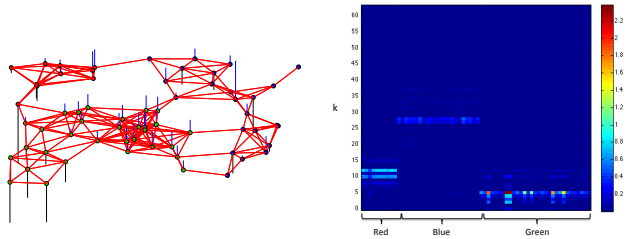

(a) (b)

Fig. 5. (a) A signal comprised of three different graph Laplacian eigenvectors restricted to three different clusters of a random sensor network. Positive components of the signal are in blue, and negative components are in black. (b) The spectrogram shows the different frequency components in the red, blue, and green clusters.

with N vertices, which are the basis vectors in the DCT-II transform [5], are $\chi_0(n) = \frac{1}{\sqrt{N}}$, $\forall n \in \{1, 2, \ldots, N\}$, and $\chi_\ell(n) = \sqrt{\frac{2}{N}} \cos\left(\frac{\pi \ell (n-0.5)}{N}\right)$ for $\ell = 1, 2, \ldots, N-1$. We compose the signal shown in Figure 4(a) on the path graph by summing three signals: χ_{10} restricted to the first 60 vertices, χ_{60} restricted to the next 60 vertices, and χ_{30} restricted to the final 60 vertices. We design a window g by setting $\hat{g}(\ell) = e^{-\tau \lambda_\ell}$ with $\tau = 300$ and then normalizing it so $\|g\|_2 = 1$. The "spectrogram" in Figure 4(b) shows $|Sf(i,k)|^2$ for all $i \in \{1, 2, \ldots, 180\}$ and $k \in \{0, 1, \ldots, 179\}$. Consistent with the intuition from discrete-time signal processing, the spectrogram shows the discrete cosines at different frequencies with the appropriate spatial localization.

In the second example, we repeat the first example on a more general graph, which is a random sensor network with 64 vertices. Using spectral clustering, we partition the network into three sets of vertices, which are shown in red, blue, and green in Figure 5(a). We take a signal f to be the sum of three signals: χ_{10} restricted to the red set of vertices, χ_{27} restricted to the blue set of vertices, and χ_5 restricted to the green set of vertices. We use the same window as above with $\tau = 3$ as the heat kernel parameter. Once again, the spectrogram, shown in Figure 5(b), elucidates the structure of f, as we can clearly see the three different frequency components present in each of the three clusters of vertices.

In the third example, we consider the graph with 1000 points sampled from the 2-D "Swiss roll" manifold, with the weights constructed as in [1, Section 8.2]. We take the window g as in the previous two examples with $\tau = 5$. In Figure 6, we show two different atoms in both the vertex and graph spectral domains.

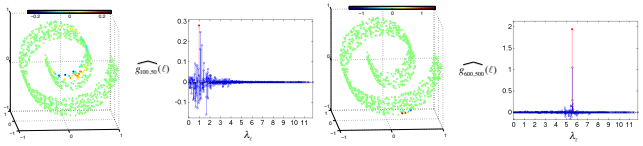

(a) (b) (c) (d)

Fig. 6. (a) The windowed graph Fourier atom $g_{100,50}$. (b) The spectral representation $\widehat{g_{100,50}}$ of the same atom. Note that $\lambda_{50} = 0.95$. (c) The atom $g_{600,500}$ in the vertex domain. (d) $g_{600,500}$ in the graph spectral domain. Note that $\lambda_{500} = 5.53$. These atoms are localized in both the vertex and graph spectral domains.

8. CONCLUSION AND FUTURE WORK

We defined generalized notions of translation and modulation through multiplication with a graph Laplacian eigenvector in the graph spectral and vertex domains, respectively. We leveraged these generalized operators to design a windowed graph Fourier transform, which enables vertex-frequency analysis for signals on graphs. When the chosen window is localized around zero in the graph spectral domain, we showed that the modulation operator is close to a translation in the graph spectral domain. If we apply this windowed graph Fourier transform to a signal with frequency components that vary along a path graph, the resulting spectrogram matches our intuition from classical discrete-time signal processing. Yet, our construction is fully generalized and can be applied to analyze signals on any undirected, connected, weighted graph. The example in Figure 5 shows that the windowed graph Fourier transform may be a valuable tool for extracting information from signals on graphs, as structural properties of the data that are hidden in the vertex domain may become obvious in the transform domain.

As ongoing work, we are i) studying ways to compute bounds on the frame in order to reconstruct a signal from its windowed graph Fourier coefficients via the frame algorithm (see, e.g., [3, Chapter 5.1.3]), ii) investigating computationally efficient methods to apply the windowed graph Fourier transform and its adjoint without explicitly computing the graph Laplacian eigenvectors, and iii) designing windows whose mathematical properties, in conjunction with structural properties of the underlying graph, can be formally linked to properties of the transform coefficients.

9. REFERENCES

[1] D. K. Hammond, P. Vandergheynst, and R. Gribonval, "Wavelets on graphs via spectral graph theory," *Appl. Comput. Harmon. Anal.*, vol. 30, no. 2, pp. 129–150, Mar. 2011.

[2] S. K. Narang and A. Ortega, "Perfect reconstruction two-channel wavelet filter-banks for graph structured data," *ArXiv e-prints*, Jun. 2011.

[3] S. G. Mallat, *A Wavelet Tour of Signal Processing*, Academic Press, 2008.

[4] F. K. Chung, *Spectral Graph Theory*, Vol. 92 of the CBMS Regional Conference Series in Mathematics, AMS Bokstore, 1997.

[5] G. Strang, "The discrete cosine transform," *SIAM Review*, vol. 41, no. 1, pp. 135–147, 1999.